



Full Length Article

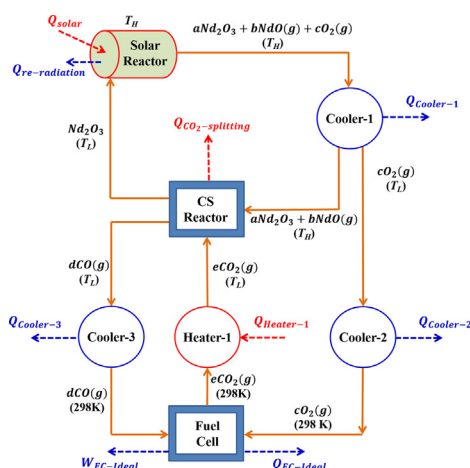
Production of solar CO via two-step neodymium oxide based thermochemical CO₂ splitting cycle

Rahul R. Bhosale

Department of Chemical Engineering, College of Engineering, Qatar University, Doha, Qatar



GRAPHICAL ABSTRACT



ARTICLE INFO

Keywords:

Neodymium oxide
CO₂ splitting
Thermal reduction
Solar CO
Thermal analysis
Process efficiency

ABSTRACT

Detailed thermodynamic scrutiny of the solar thermochemical neodymium oxide-based CO₂ splitting (Nd-CS) cycle is reported. The thermal reduction (TR) and CO₂ splitting (CS) reaction temperatures required for the operation of the Nd-CS cycle were determined. The equilibrium compositions of Nd₂O₃, NdO, and O₂ exhibit that the initiation of the TR of Nd₂O₃ is feasible at 1982 K, and the complete conversion is possible at 2232 K. As per the delta G analysis, the CS reaction was feasible at all temperatures above 300 K. After understanding the chemical thermodynamic equilibrium of the Nd-CS cycle, the efficiency analysis was performed by using the HSC Chemistry 9.9 software. The results obtained via the efficiency analysis shows that the Nd-CS cycle was capable of attaining the highest possible $\eta_{\text{solar-to-fuel-Nd-CS}} = 9.45\%$ at partial TR of Nd₂O₃ = 55% ($T_H = 2154$ K). Application of HR = 20%, 40%, 60%, 80%, and 100%, improved $\eta_{\text{solar-to-fuel-Nd-CS}}$ at TR-Nd = 55% ($T_H = 2154$ K) up to 10.51%, 11.84%, 13.55%, 15.85%, and 19.09%, respectively.

1. Introduction

Production of transportation fuels such as gasoline, diesel, kerosene, and others from syngas can be achieved via a catalytic Fischer-Tropsch

Process [1]. Typically, fossil fuels are converted into syngas via the reforming process. Although this is a proven technology, the emissions associated with fossil fuel utilization are considered as one of the primary sources for climate contamination, such as global warming [2–5].

E-mail address: rahul.bhosale@qu.edu.qa.

<https://doi.org/10.1016/j.fuel.2020.118803>

Received 24 April 2020; Received in revised form 26 June 2020; Accepted 21 July 2020

Available online 31 July 2020

0016-2361/ © 2020 Elsevier Ltd. All rights reserved.

Nomenclature

C	Solar flux concentration ratio, suns
HHV	Higher heating value, kW
I	Normal beam solar insolation, W/m ²
MO	Metal oxide
\dot{n}	Molar flow rate, mol/s
T_H	TR temperature, K
T_L	Water splitting temperature, K
HR	Heat recuperation
P_{O_2}	The partial pressure of the O ₂ in the inert gas, atm
σ	Stefan – Boltzmann constant, 5.670×10^{-8} (W/m ² ·K ⁴)
$\dot{Q}_{Nd_2O_3-red(partial)-Nd-CS}$	Energy required for partial reduction of Nd ₂ O ₃ (Nd-CS cycle), kW
$\dot{Q}_{CO_2-heating-Nd-CS}$	Energy required for the heating of CO ₂ (Nd-CS cycle), kW
$\dot{Q}_{cycle-net-Nd-CS}$	Net energy required to run the Nd-CS cycle, kW
$\dot{Q}_{solar-reactor-Nd-CS}$	Solar energy required to run the solar reactor (Nd-CS cycle), kW
$\dot{Q}_{solar-heater-Nd-CS}$	Solar energy required to run the solar heater (Nd-CS cycle), kW
$\dot{Q}_{solar-cycle-Nd-CS}$	Solar energy required to run the Nd-CS cycle, kW
$\eta_{abs-solar-reactor-Nd-CS}$	Solar energy absorption efficiency of the solar reactor (Nd-CS cycle), %

$\eta_{abs-solar-heater-Nd-CS}$	Solar energy absorption efficiency of the solar heater (Nd-CS cycle), %
$\dot{Q}_{re-rad-solarreactor-Nd-CS}$	Re-radiation losses from the solar reactor (Nd-CS cycle), kW
$\dot{Q}_{re-rad-solar-heater-Nd-CS}$	Re-radiation losses from the solar heater (Nd-CS cycle), kW
$\dot{Q}_{re-rad-cycle-Nd-CS}$	Re-radiation losses from the Nd-CS cycle, kW
$\dot{Q}_{cooler-1-Nd-CS}$	Energy liberated from cooler – 1 (Nd-CS cycle), kW
$\dot{Q}_{cooler-2-Nd-CS}$	Energy liberated from cooler – 2 (Nd-CS cycle), kW
$\dot{Q}_{cooler-3-Nd-CS}$	Energy liberated from cooler – 3 (Nd-CS cycle), kW
$\dot{Q}_{splitting-reactor-Nd-CS}$	Energy liberated from the CO ₂ splitting reactor (Nd-CS cycle), kW
$\dot{Q}_{FC-Ideal-Nd-CS}$	Energy liberated from an ideal fuel cell (Nd-CS cycle), kW
$\dot{W}_{FC-Ideal-Nd-CS}$	Work output of an ideal fuel cell (Nd-CS cycle), kW
$\eta_{solar-to-fuel-Nd-CS}$	Solar-to-fuel energy conversion efficiency (Nd-CS cycle), %
$\eta_{solar-to-fuel-HR-Nd-CS}$	Solar-to-fuel energy conversion efficiency (with heat recuperation, Nd-CS cycle), %
$\dot{Q}_{recuperable-Nd-CS}$	Total energy recuperated from the Nd-CS cycle, kW
$\dot{Q}_{recupaerable-HR-Nd-CS}$	Energy recuperated from the Nd-CS cycle (with % HR), kW
$\dot{Q}_{solar-cycle-HR-Nd-CS}$	Solar energy required to run the Nd-CS cycle (with heat recuperation), kW

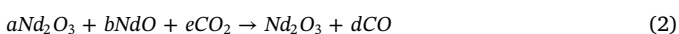
Hence, it is highly essential to identify new ways for the production of syngas, i.e., a mixture of H₂ and CO.

H₂ and CO generation via a metal oxide (MO) based solar thermochemical cycle (STC) is one of the promising options that can be considered as a replacement for fossil fuel utilization towards syngas production [6–9]. The MOs can be applied for both water splitting (WS) as well as CO₂ splitting (CS) reactions. Below is the list of MOs used for the STCs in previous studies.

- Iron Oxide [10–12]
- Zinc Oxide [13–15]
- Tin Oxide [16,17]
- Ferrites [18–24]
- Ceria and doped ceria [25–31]
- Perovskites [7,31–36]

In addition to the above mentioned MOs, recently, lanthanide-based oxides such as samarium oxide [37,38], terbium oxide [39], and erbium oxide [38,40] were also explored for the STCs. Similar to the samarium, terbium, and erbium, the neodymium (Nd) was also utilized as an active dopant in the case of the ceria materials and other H₂ generation techniques. As neodymium is proved to be an active catalytic material beneficial for various processes, it is believed that the neodymium oxide (Nd₂O₃) will be useful also for the production of H₂ and CO via WS and CS reactions. It is important to note that the Nd₂O₃ is not yet investigated as a MO for the STCs.

In this study, attempts were made to investigate the feasibility of the neodymium oxide-based CO₂ splitting (Nd-CS) cycle by performing a thermodynamic equilibrium and efficiency analysis. HSC Chemistry software 9.9 was utilized as the source for gathering the material properties necessary for the thermodynamic calculations. All computations were carried out by assuming partial TR of Nd₂O₃ (TR-Nd). The redox equations associated with the partially reduced two-step Nd-CS cycle are as follows:



2. Equilibrium analysis, process flow configuration, and modeling equations

HSC Chemistry provides an easy and quick approach for the thermodynamic analysis. HSC Chemistry is especially useful for the exploration of the effect of different variables on chemical processes at equilibrium conditions. The HSC name was given to the software as it is capable of performing the calculations by utilizing the thermochemical database related to enthalpy (H), entropy (S), and heat capacity (Cp) for more than 28,000 chemical species (equivalent to more than twenty thick data books). Due to all these advantages, HSC has a wide range of applications in scientific education, industry, and research. Hence, in this study, the thermodynamic scrutiny of the Nd-CS cycle was performed by using the HSC Chemistry 9.9 software.

Estimation of the equilibrium compositions and temperatures associated with the thermal reduction (TR) and CO₂ splitting (CS) reactions is an essential step towards performing the efficiency analysis of an STC. Therefore, as an initial step, the thermodynamic equilibrium analysis of the solar-driven Nd-CS cycle was conducted. The equilibrium analysis was carried out by assuming a $P_{O_2} = 10^{-6}$ atm. Fig. 1 represents the equilibrium compositions related to the thermal

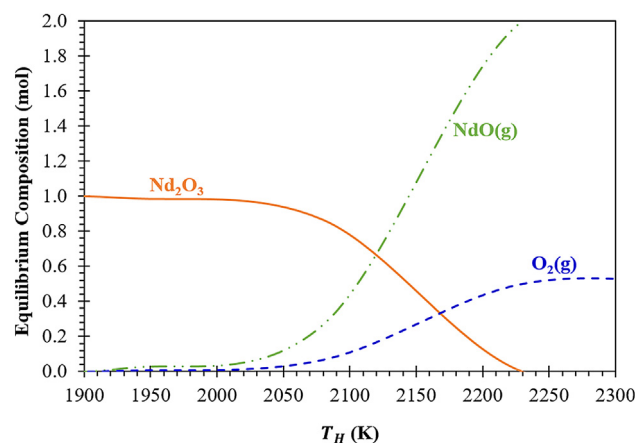


Fig. 1. Equilibrium compositions allied with the TR of Nd₂O₃.

decomposition of Nd_2O_3 as a function of change in the TR temperature (T_H). The reported equilibrium compositions of Nd_2O_3 , NdO , and O_2 show that the initiation of the TR of Nd_2O_3 is feasible at 1982 K. It was also understood that the complete conversion of Nd_2O_3 is possible at 2232 K.

As this investigation was focused on understanding the influence of partial TR of Nd_2O_3 (TR-Nd) on the solar-to-fuel energy conversion efficiency of the Nd-CS cycle, it was necessary to identify the exact T_H at which the TR-Nd varies in the range of 5% to 100%. The T_H required for the partial TR-Nd was recognized by using the equilibrium compositions reported in Fig. 1. The results reported in Fig. 2 shows the variation in the T_H required for a specific partial TR-Nd. According to the trend reported, for an initial rise in the TR-Nd from 5% to 15%, the T_H increased sharply from 1982 K to 2086 K. For further upsurge in the TR-Nd from 15% to 100%, the T_H surged linearly with a slow increase. For example, to raise the TR-Nd from 15% to 30%, 45%, 60%, and 75%, and 90%, the T_H amplified from 2086 K up to 2112 K, 2137 K, 2163 K, and 2189 K, respectively (Fig. 3).

The estimation of T_L , which was necessary for performing the re-oxidation of NdO via CS reaction, was the next important step of the equilibrium analysis. T_L above which the complete re-oxidation of NdO to Nd_2O_3 is possible was determined by exploring the variations associated with the delta G of the CS reaction. According to the numbers, the CS reaction associated with the Nd-CS cycle was feasible at all temperatures above 300 K. To understand the viability of the Nd-CS cycle, it was vital to compare the obtained results with the previously investigated thermochemical CS cycles. The published literature shows that in most of the CS studies, the re-oxidation of the MO via CS reaction was carried out at ~ 1300 K [25,33]. Hence, to have a fair comparison, the re-oxidation of NdO via CS reaction was performed at $T_L = 1300$ K.

After performing the equilibrium analysis, a detailed process flow configuration of the Nd-CS cycle was developed. The TR and CS reactions associated with the Nd-CS cycle were conducted in a solar-driven cavity-based reactor and the non-solar CS reactor. The preheating of the CO_2 from 298 K up to T_L was achieved in a solar-driven CO_2 heater. The temperatures of a) the products exiting the solar reactor (after TR step), b) the CO coming out of the CS reactor, and c) the CO_2 before entering the CS reactor were maintained at the respective required values with the help of the three coolers. Besides, an ideal fuel cell (with assumed 100% efficiency) was placed in the cycle to determine the work output of the CO produced. All the thermodynamic calculations carried out by assuming a constant feed rate of Nd_2O_3 to the solar reactor (1 mol/s), negligible conductive/convective heat and viscous losses from the solar reactor, insignificant variations in the kinetic as well as potential energies, complete conversion of CO_2 into CO, and natural separation of the products associated with the TR and CS reactions. The thermodynamic properties gathered from the HSC Chemistry 9.9 software. The computations allied with the heat exchangers not considered in the thermodynamic analysis.

As the initial step of the efficiency analysis, the solar absorption efficiencies for the solar reactor and the solar heater determined as follows:

$$\eta_{\text{abs-solar-reactor-Nd-CS}} = 1 - \left(\frac{\sigma T_H^4}{IC} \right) \quad (3)$$

$$\eta_{\text{abs-solar-heater-Nd-CS}} = 1 - \left(\frac{\sigma T_L^4}{IC} \right) \quad (4)$$

where, $I = 1000 \text{ W/m}^2$, $C = 3000 \text{ suns}$, $\sigma = 5.670 \times 10^{-8} \text{ W/m}^2\text{K}^4$.

The solar energy needed to drive the solar reactor, and the solar heater was estimated as:

$$\dot{Q}_{\text{solar-reactor-Nd-CS}} = \frac{\dot{Q}_{\text{Nd}_2\text{O}_3\text{-red(partial)-Nd-CS}}}{\eta_{\text{abs-solar-reactor-Nd-CS}}} \quad (5)$$

$$\dot{Q}_{\text{solar-heater-Nd-CS}} = \frac{\dot{Q}_{\text{CO}_2\text{-heating-Nd-CS}}}{\eta_{\text{abs-solar-heater-Nd-CS}}} \quad (6)$$

where

$$\dot{Q}_{\text{Nd}_2\text{O}_3\text{-red(partial)-Nd-CS}} = \dot{n}\Delta H|_{\text{Nd}_2\text{O}_3(\text{s})@T_L \rightarrow a\text{Nd}_2\text{O}_3(\text{s})+b\text{NdO}(\text{g})+c\text{O}_2(\text{g})@T_H} \quad (7)$$

$$\dot{Q}_{\text{CO}_2\text{-heating-Nd-CS}} = \dot{n}\Delta H|_{e\text{CO}_2(\text{g})@298\text{K} \rightarrow e\text{CO}_2(\text{g})@T_L} \quad (8)$$

$\dot{Q}_{\text{cycle-net-Nd-CS}}$ was calculated by adding Eqs. (7) and (8).

$$\dot{Q}_{\text{cycle-net-Nd-CS}} = \dot{Q}_{\text{Nd}_2\text{O}_3\text{-red(partial)-Nd-CS}} + \dot{Q}_{\text{CO}_2\text{-heating-Nd-CS}} \quad (9)$$

Similarly, $\dot{Q}_{\text{solar-cycle-Nd-CS}}$ was valued by summing Eqs. (5) and (6) together.

$$\dot{Q}_{\text{solar-cycle-Nd-CS}} = \dot{Q}_{\text{solar-reactor-Nd-CS}} + \dot{Q}_{\text{solar-heater-Nd-CS}} \quad (10)$$

The heat losses associated with the solar reactor and solar heater, due to the re-radiation, were computed as follows:

$$\dot{Q}_{\text{re-rad-solar-reactor-Nd-CS}} = \dot{Q}_{\text{solar-reactor-Nd-CS}} - \dot{Q}_{\text{Nd}_2\text{O}_3\text{-red(partial)-Nd-CS}} \quad (11)$$

$$\dot{Q}_{\text{re-rad-solar-heater-Nd-CS}} = \dot{Q}_{\text{solar-heater-Nd-CS}} - \dot{Q}_{\text{CO}_2\text{-heating-Nd-CS}} \quad (12)$$

With the help of Eqs. (11) and (12), $\dot{Q}_{\text{re-rad-cycle-Nd-CS}}$ was determined as:

$$\dot{Q}_{\text{re-rad-cycle-Nd-CS}} = \dot{Q}_{\text{re-rad-solar-reactor-Nd-CS}} + \dot{Q}_{\text{re-rad-solar-heater-Nd-CS}} \quad (13)$$

$\eta_{\text{solar-to-fuel-Nd-CS}}$ of the Nd-CS cycle was calculated as per the following expression:

$$\eta_{\text{solar-to-fuel-Nd-CS}} = \frac{\text{HHV}_{\text{CO}} \times (\text{moles of CO produced})}{\dot{Q}_{\text{solar-cycle-Nd-CS}}} \quad (14)$$

The influence of heat recuperation on the process efficiency was evaluated by estimating $\eta_{\text{solar-to-fuel-HR-Nd-CS}}$.

$$\eta_{\text{solar-to-fuel-HR-Nd-CS}} = \frac{\text{HHV}_{\text{CO}} \times (\text{moles of CO produced})}{\dot{Q}_{\text{solar-cycle-HR-Nd-CS}}} \quad (15)$$

For the determination of $\eta_{\text{solar-to-fuel-HR-Nd-CS}}$, estimation of the total amount of heat that recuperated from the Nd-CS cycle was essential. Hence, $\dot{Q}_{\text{solar-cycle-HR-Nd-CS}}$ was computed as per the following equation.

$$\begin{aligned} \dot{Q}_{\text{recuperable-Nd-CS}} &= \dot{Q}_{\text{cooler-1-Nd-CS}} + \dot{Q}_{\text{cooler-2-Nd-CS}} + \dot{Q}_{\text{cooler-3-Nd-CS}} \\ &+ \dot{Q}_{\text{splitting-reactor-Nd-CS}} \end{aligned} \quad (16)$$

As per Eq. (16), $\dot{Q}_{\text{recuperable-Nd-CS}}$ can be calculated if the values for

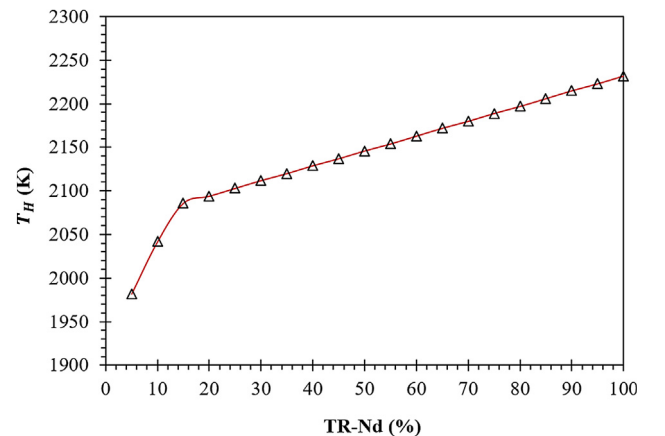


Fig. 2. T_H required for the partial TR of Nd_2O_3 .

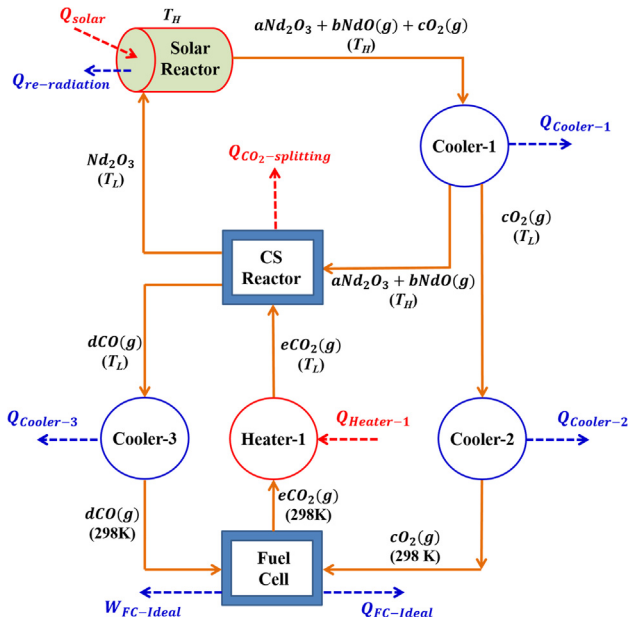


Fig. 3. Process flow arrangement for the Nd-CS cycle.

the energy released by the coolers and the CS reactor are known.

$$\dot{Q}_{\text{cooler-1-Nd-CS}} = -\dot{n}\Delta H|_{aNd_2O_3(s)+bNdO(g)+cO_2(g)@T_H \rightarrow aNd_2O_3(s)+bNdO(s)+cO_2(g)@T_L} \quad (17)$$

$$\dot{Q}_{\text{cooler-2-Nd-CS}} = -\dot{n}\Delta H|_{cO_2(g)@T_L \rightarrow cO_2(g)@298K} \quad (18)$$

$$\dot{Q}_{\text{cooler-3-Nd-CS}} = -\dot{n}\Delta H|_{dCO(g)@T_L \rightarrow dCO(g)@298K} \quad (19)$$

$$\dot{Q}_{\text{splitting-reactor-Nd-CS}} = -\dot{n}\Delta H|_{aNd_2O_3(s)+bNdO(s)+eCO_2(g)@T_L \rightarrow Nd_2O_3(s)+dCO(g)@T_L} \quad (20)$$

The total amount of solar energy needed to drive the Nd-CS cycle after applying the heat recuperation was estimated as:

$$\dot{Q}_{\text{solar-cycle-HR-Nd-CS}} = \dot{Q}_{\text{solar-cycle-Nd-CS}} - \dot{Q}_{\text{recuperable-HR-Nd-CS}} \quad (21)$$

Where

$$\dot{Q}_{\text{recuperable-HR-Nd-CS}} = (\%HR) \times \dot{Q}_{\text{recuperable-Nd-CS}} \quad (22)$$

The $\dot{W}_{FC-Ideal}$ was calculated as per Eqs. (23) as well as (24) and compared for the verification of the analysis performed in this study.

$$\dot{W}_{FC-Ideal-Nd-CS} = -\dot{n}\Delta G|_{dCO(g)+cO_2(g)@298K \rightarrow eCO_2(g)@298K} \quad (23)$$

$$\begin{aligned} \dot{W}_{FC-Ideal-Nd-CS} &= \dot{Q}_{\text{solar-cycle-Nd-CS}} - \\ &(\dot{Q}_{\text{re-rad-cycle-Nd-CS}} + \dot{Q}_{\text{cooler-1-Nd-CS}} + \dot{Q}_{\text{cooler-2-Nd-CS}} \\ &+ \dot{Q}_{\text{cooler-3-Nd-CS}} + \dot{Q}_{\text{splitting-reactor-Nd-CS}} + \dot{Q}_{FC-Ideal-Nd-CS}) \end{aligned} \quad (24)$$

where

$$\dot{Q}_{FC-Ideal-Nd-CS} = -(298) \times \dot{n}\Delta S|_{dCO(g)+cO_2(g)@298K \rightarrow eCO_2(g)@298K} \quad (25)$$

3. Results and discussion

3.1. Solar reactor and heater

The thermodynamic efficiency analysis associated with the Nd-CS cycle conducted by utilizing the equations listed in section 2. The thermodynamic data obtained from the HSC Chemistry 9.9 software. As mentioned in section 2, T_H required for the rise in the partial TR-Nd

Table 1

Effect of the %TR-Nd on $\dot{Q}_{Nd_2O_3-red(partial)-Nd-CS}$ and $\dot{Q}_{CO_2-heating-Nd-CS}$.

%TR-Nd	$\dot{Q}_{Nd_2O_3-red(partial)-Nd-CS}$ (kW)	$\dot{Q}_{CO_2-heating-Nd-CS}$ (kW)
5	185.3	2.5
10	270.4	5.0
15	352.5	7.5
20	428.7	10.0
25	505.1	12.5
30	581.3	15.1
35	657.4	17.6
40	733.6	20.1
45	809.6	22.6
50	885.7	25.1
55	961.5	27.6
60	1037.5	30.1
65	1113.5	32.6
70	1189.2	35.1
75	1265.1	37.6
80	1340.7	40.1
85	1416.4	42.7
90	1492.1	45.2
95	1567.6	47.7
100	1643.2	50.2

from 15% to 30%, 45%, 60%, 75%, and 90% increased from 2086 K up to 2112 K, 2137 K, 2163 K, 2189 K, and 2215 K, respectively. This enhancement in T_H resulted in a reduction in the $\eta_{\text{abs-solar-reactor-Nd-CS}}$. For example, $\eta_{\text{abs-solar-reactor-Nd-CS}}$ decreased from 64.2% to 62.4%, 60.6%, 58.6%, 56.6%, and 54.5% when the TR-Nd rose from 15% to 30%, 45%, 60%, 75%, and 90%, respectively. Although $\eta_{\text{abs-solar-reactor-Nd-CS}}$ was reduced considerably as a function of the rise in the %TR-Nd, $\eta_{\text{abs-solar-heater-Tb-CS}}$ however, remained unchanged at 94.5% as the CS step was carried out at a constant $T_L = 1300$ K.

The estimation of the solar reactor and solar heater absorption efficiencies was necessary for the calculation of $\dot{Q}_{\text{solar-reactor-Nd-CS}}$ and $\dot{Q}_{\text{solar-heater-Nd-CS}}$. In addition to the solar absorption efficiency values, $\dot{Q}_{Nd_2O_3-red(partial)-Nd-CS}$ and $\dot{Q}_{CO_2-heating-Nd-CS}$ can also affect the $\dot{Q}_{\text{solar-reactor-Nd-CS}}$ and $\dot{Q}_{\text{solar-heater-Nd-CS}}$ significantly. Hence, before calculating $\dot{Q}_{\text{solar-reactor-Nd-CS}}$ and $\dot{Q}_{\text{solar-heater-Nd-CS}}$, the variations allied with $\dot{Q}_{Nd_2O_3-red(partial)-Nd-CS}$ and $\dot{Q}_{CO_2-heating-Nd-CS}$ as a function of the rise in %TR-Nd was computed. As shown in Table 1, both $\dot{Q}_{Nd_2O_3-red(partial)-Nd-CS}$ and $\dot{Q}_{CO_2-heating-Nd-CS}$ upsurged due to the rise in the %TR-Nd. $\dot{Q}_{Nd_2O_3-red(partial)-Nd-CS}$ was increased from 352.5 kW by a factor of 1.6, 2.3, 2.9, 3.6, and 4.2 when the TR-Nd rose from 15% to 30%, 45%, 60%, 75%, and 90%, respectively. This rise in $\dot{Q}_{Nd_2O_3-red(partial)-Nd-CS}$ was apparent as higher energy input was needed to upturn %TR-Nd from 5% to 100%.

As %TR-Nd was increased from 5% to 100%, a higher quantity of O_2 was released, which improved the chances of production of higher levels of CO via CS reaction. To achieve an elevated CO production, more quantity of CO_2 was fed to the CS reactor, which resulted in a rise in $\dot{Q}_{CO_2-heating-Nd-CS}$. In terms of numbers, the increase in the TR-Nd from 15% to 30%, 45%, 60%, 75%, and 90% enhanced $\dot{Q}_{CO_2-heating-Nd-CS}$ from 7.5 kW up to 15.1 kW, 22.6 kW, 30.1 kW, 37.6 kW, and 45.2 kW, respectively.

With the help of Eqs. (5) and (6), $\dot{Q}_{\text{solar-reactor-Nd-CS}}$ and $\dot{Q}_{\text{solar-heater-Nd-CS}}$ were calculated and presented in Fig. 4. According to Eq. (5), $\dot{Q}_{\text{solar-reactor-Nd-CS}}$ is a ratio of $\dot{Q}_{Nd_2O_3-red(partial)-Nd-CS}$ over $\eta_{\text{abs-solar-reactor-Nd-CS}}$. As mentioned in the previous paragraphs, with a rise in %TR-Nd, $\dot{Q}_{Nd_2O_3-red(partial)-Nd-CS}$ was increased, whereas the $\eta_{\text{abs-solar-reactor-Tb-CS}}$ was decreased. Subsequently, $\dot{Q}_{\text{solar-reactor-Nd-CS}}$ was upsurged as a function of an upturn in the %TR-Nd. For example, as the TR-Nd was enhanced from 15% to 30%, 45%, 60%, 75%, and 90%, $\dot{Q}_{\text{solar-reactor-Nd-CS}}$ was amplified above 549.0 kW by 382.7 kW, 787.4 kW, 1220.8 kW, 1686.1 kW, and 2188.8 kW, respectively (Fig. 4a).

Eq. (6) indicates that the $\dot{Q}_{CO_2-heating-Nd-CS}$ divided by $\eta_{\text{abs-solar-heater-Nd-CS}}$ equal to $\dot{Q}_{\text{solar-heater-Nd-CS}}$. As per the obtained

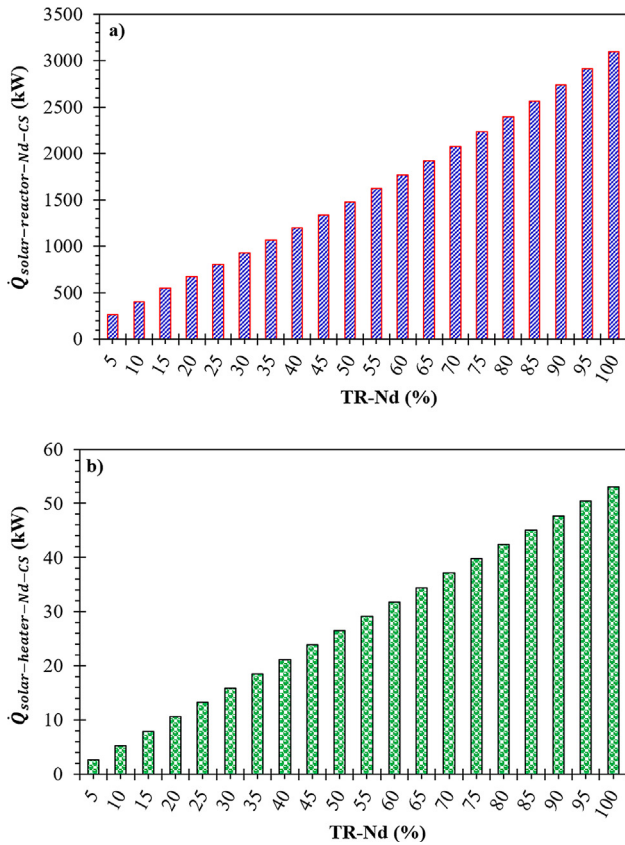


Fig. 4. Effect of %TR-Nd on a) $\dot{Q}_{solar-reactor-Nd-CS}$ and b) $\dot{Q}_{solar-heater-Nd-CS}$.

results, the $\dot{Q}_{CO_2-heating-Nd-CS}$ enhanced when the %TR-Nd improved from 5% to 100%. In contrast, the $\eta_{abs-solar-heater-Nd-CS}$ stayed unchanged at all values of %TR-Nd. Hence, as only $\dot{Q}_{CO_2-heating-Nd-CS}$ increased, the rise in the $\dot{Q}_{solar-heater-Nd-CS}$ was considerably less when compared to the $\dot{Q}_{solar-reactor-Nd-CS}$. For instance, the $\dot{Q}_{solar-heater-Nd-CS}$ augmented up to 8.0 kW, 15.9 kW, 23.9 kW, 31.8 kW, 39.8 kW, and 47.7 kW at TR-Nd = 15%, 30%, 45%, 60%, 75%, and 90%, respectively (Fig. 4b).

Fig. 5 represents the variations associated with $\dot{Q}_{cycle-net-Nd-CS}$ and $\dot{Q}_{solar-cycle-Nd-CS}$ due to the increment in %TR-Nd. According to Eq. (9), $\dot{Q}_{cycle-net-Nd-CS}$ is the addition of $\dot{Q}_{Nd_2O_3-red(partial)-Nd-CS}$ and $\dot{Q}_{CO_2-heating-Nd-CS}$. Similarly, the summation of $\dot{Q}_{solar-reactor-Nd-CS}$ and $\dot{Q}_{solar-heater-Nd-CS}$ together is equal to $\dot{Q}_{solar-cycle-Nd-CS}$. As reported in the previous paragraphs, as $\dot{Q}_{Nd_2O_3-red(partial)-Nd-CS}$, $\dot{Q}_{CO_2-heating-Nd-CS}$, $\dot{Q}_{solar-reactor-Nd-CS}$, and $\dot{Q}_{solar-heater-Nd-CS}$ was upsurged, $\dot{Q}_{cycle-net-Nd-CS}$ and $\dot{Q}_{solar-cycle-Nd-CS}$ was also enhanced.

As shown in Fig. 5, $\dot{Q}_{cycle-net-Nd-CS}$ was increased from 360.1 kW up to 596.4 kW, 832.2 kW, 1067.6 kW, 1302.7 kW, and 1537.3 kW when the TR-Nd amplified from 15% to 30%, 45%, 60%, 75%, and 90%, respectively. Likewise, $\dot{Q}_{solar-cycle-Nd-CS}$ was upsurged above 557.0 kW by 390.7 kW, 803.3 kW, 1244.6 kW, 1717.9 kW, and 2228.6 kW as the TR-Nd was enlarged from 15% to 30%, 45%, 60%, 75%, and 90%, respectively. $\dot{Q}_{solar-cycle-Nd-CS}$ was higher than $\dot{Q}_{cycle-net-Nd-CS}$ due to the reduction in $\eta_{abs-solar-reactor-Tb-CS}$ as a function of the increase in %TR-Nd.

3.2. Re-radiation losses

As per the assumptions, the conductive and convective heat losses from the solar reactor and solar heater were negligible. However, the heat losses from these solar equipments due to re-radiation through the cavity window needs to be considered during the efficiency analysis. The re-radiation losses from the solar reactor occurred due to the

reduction in $\eta_{abs-solar-reactor-Nd-CS}$ as a function of %TR-Nd. As per the calculations performed using Eq. (11), $\dot{Q}_{re-rad-solar-reactor-Nd-CS}$ was increased from 196.5 kW up to 350.4 kW, 526.8 kW, 732.3 kW, 970.1 kW, and 1245.8 kW due to the increment in the TR-Nd from 15% to 30%, 45%, 60%, 75%, and 90%, respectively.

As the working temperature of the solar heater was steady at 1300 K, the $\eta_{abs-solar-heater-Nd-CS}$ was remained constant at 94.6%. Hence, the re-radiation losses occurred only because of the temperature difference between the working and ambient temperatures. In terms of numbers, the rise in the TR-Nd from 15% to 30%, 45%, 60%, 75%, and 90% increased the $\dot{Q}_{re-rad-solar-heater-Nd-CS}$ from 0.43 kW to 0.86 kW, 1.29 kW, 1.72 kW, 2.15 kW, and 2.58 kW, respectively.

Table 2 reports the overall re-radiation losses from the Nd-CS cycle calculated as per Eq. (13). As mentioned in the Eq. (13), $\dot{Q}_{re-rad-cycle-Nd-CS}$ is the summation of $\dot{Q}_{re-rad-solar-reactor-Nd-CS}$ and $\dot{Q}_{re-rad-solar-heater-Nd-CS}$ together. As $\dot{Q}_{re-rad-solar-reactor-Nd-CS}$ and $\dot{Q}_{re-rad-solar-heater-Nd-CS}$ increased, $\dot{Q}_{re-rad-cycle-Nd-CS}$ also upsurged as a function of %TR-Nd. In terms of numbers reported in Table 2, $\dot{Q}_{re-rad-cycle-Nd-CS}$ was surged above 196.9 kW by a factor of 1.8, 2.7, 3.7, 4.9, and 6.3 when the TR-Nd amplified from 15% to 30%, 45%, 60%, 75%, and 90%, respectively.

3.3. Coolers and CS reactor

For the estimation of the total amount of energy that can be recuperable from the Nd-CS cycle, it was necessary first to understand the amount of heat energy dissipated by the coolers and the CS reactor. Eqs. (17)–(20) were applied for the estimation of $\dot{Q}_{cooler-1-Nd-CS}$, $\dot{Q}_{cooler-2-Nd-CS}$, $\dot{Q}_{cooler-3-Nd-CS}$, and $\dot{Q}_{splitting-reactor-Nd-CS}$.

As shown in the process flow diagram, the cooler-1 was installed in the Nd-CS cycle for reducing the temperature of the mixture containing Nd_2O_3 , NdO, and O_2 from T_H to T_L . The data presented in Fig. 2 shows that to achieve a higher %TR-Nd, elevated T_H was needed. As the T_H upsurged from 1982 K to 2232 K, the difference between the T_H and T_L was increased. This rise in T_H and T_L temperature gap resulted in greater heat dissipation from the cooler-1. The results presented in Fig. 6 shows that $\dot{Q}_{cooler-1-Nd-CS}$ was increased from 135.2 kW by 11.5 kW, 22.4 kW, 33.0 kW, 43.1 kW, and 52.9 kW due to the rise in the TR-Nd from 15% up to 30%, 45%, 60%, 75%, and 90%, respectively.

Similar to the cooler-1, the heat energy released by cooler-2 and cooler-3 was also enhanced as a function of the increment in %TR-Nd. This happens due to a) release of a higher quantity of O_2 during the TR step and b) production of elevated levels of CO during the CS step. In terms of numbers, $\dot{Q}_{cooler-2-Nd-CS}$ was increased from 0.8 kW to 16.7 kW, and $\dot{Q}_{cooler-3-Nd-CS}$ was enhanced from 1.6 kW to 31.9 kW due to the upsurge in the TR-Nd from 5% to 100%, respectively.

In addition to the three coolers, the CS reactor also emits heat energy due to the exothermic nature of the CS reaction. Fig. 6 shows the variations associated with $\dot{Q}_{splitting-reactor-Nd-CS}$ as a function of the rise

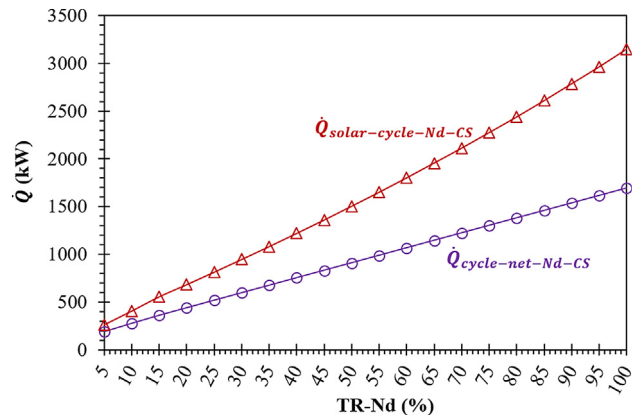


Fig. 5. Effect of %TR-Nd on $\dot{Q}_{cycle-net-Nd-CS}$ and $\dot{Q}_{solar-cycle-Nd-CS}$.

Table 2
Effect of %TR-Nd on $\dot{Q}_{re-rad-cycle-Nd-CS}$.

%TR-Nd	$\dot{Q}_{re-rad-cycle-Nd-CS}$ (kW)
5	76.5
10	132.6
15	196.9
20	245.4
25	297.0
30	351.3
35	407.1
40	466.9
45	528.1
50	594.1
55	661.3
60	734.0
65	810.5
70	887.9
75	972.2
80	1057.4
85	1150.4
90	1248.3
95	1346.8
100	1455.0

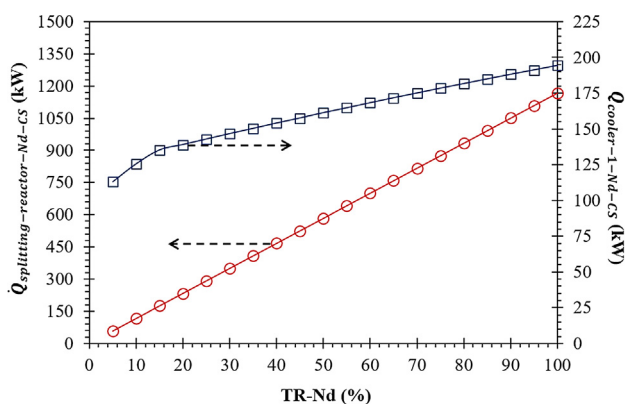


Fig. 6. Effect of %TR-Tb on $\dot{Q}_{cooler-1-Nd-CS}$ and $\dot{Q}_{splitting-reactor-Nd-CS}$.

in the %TR-Nd. The increase in %TR-Nd resulted in the release of a higher level of O_2 , which further signifies an improvement in the production of CO during the CS reaction. The exothermicity associated with the CS reaction was also enhanced, which results in an upsurge in $\dot{Q}_{splitting-reactor-Nd-CS}$. For instance, $\dot{Q}_{splitting-reactor-Nd-CS}$ was increased from 58.4 kW up to 1167.6 kW due to the upturn in the TR-Nd from 5% to 100%.

3.4. Efficiency

The judgment about the practicability of a CS cycle can be analyzed by estimating its solar-to-fuel energy conversion efficiency. Hence, after calculating the essential process parameters, the final step was to compute $\eta_{solar-to-fuel-Nd-CS}$. $\eta_{solar-to-fuel-Nd-CS}$ depends directly on the HHV of CO produced and inversely to the $\dot{Q}_{solar-cycle-Nd-CS}$. The variations associated with $\eta_{solar-to-fuel-Nd-CS}$ due to the increment in the %TR-Nd are reported in Fig. 7. $\eta_{solar-to-fuel-Nd-CS}$ was increased from 5.36% to 9.45% as the TR-Nd upsurged from 5% to 55%. A further upturn in the TR-Nd from 55% to 100% resulted in a reduction in $\eta_{solar-to-fuel-Nd-CS}$ from 9.45% to 9.00%. It was quite evident from Fig. 7 that the surge in $\eta_{solar-to-fuel-Nd-CS}$ from TR-Nd = 5% to 55% was considerably quick as compared to the drop in $\eta_{solar-to-fuel-Nd-CS}$ from TR-Nd = 55% to 100%. The results obtained further indicate that during the period of TR-Nd = 5% to 55%, the rise in the HHV of CO produced has a more pronounced impact on $\eta_{solar-to-fuel-Nd-CS}$. On the other hand, as the TR-Nd rose from 55% to 100%, the influence of the

upturn in $\dot{Q}_{solar-cycle-Nd-CS}$ became significant, and hence $\eta_{solar-to-fuel-Nd-CS}$ was reduced. Overall, the Nd-CS cycle was capable of attaining the highest $\eta_{solar-to-fuel-Nd-CS} = 9.45\%$ at TR-Nd = 55% ($T_H = 2154$ K).

As reported in the previous studies, the re-utilization of the heat energy released by the coolers and CS reactor, i.e., heat recuperation, helps to achieve a higher solar-to-fuel energy conversion efficiency. For the calculation of $\eta_{solar-to-fuel-HR-Nd-CS}$, firstly, the $\dot{Q}_{recuperable-Nd-CS}$ was calculated as per Eq. (16). The numbers obtained indicate a higher $\dot{Q}_{recuperable-Nd-CS}$ at an elevated %TR-Nd. For example, as the TR-Nd increased from 15% to 30%, 45%, 60%, 75%, and 90%, $\dot{Q}_{recuperable-Nd-CS}$ rose above 317.6 kW up to 511.5 kW, 704.8 kW, 897.9 kW, 1090.5 kW, and 1282.6 kW, respectively.

After determining $\dot{Q}_{recuperable-Nd-CS}$, the next step was to compute $\dot{Q}_{solar-cycle-HR-Nd-CS}$ as per Eq. (12). The values obtained for $\dot{Q}_{solar-cycle-HR-Nd-CS}$ as a function of the %HR and %TR-Nd are reported compared indicate that $\dot{Q}_{solar-cycle-HR-Nd-CS}$ was dropped higher as compared to $\dot{Q}_{solar-cycle-Nd-CS}$ due to the rise in %HR. For example, at TR-Nd = 20%, $\dot{Q}_{solar-cycle-HR-Nd-CS}$ at HR = 20%, 40%, 60%, 80%, and 100%, was lower than $\dot{Q}_{solar-cycle-Nd-CS}$ by 11.2%, 22.3%, 33.5%, 44.7%, and 55.9%, respectively. Likewise, at TR-Nd = 80%, $\dot{Q}_{solar-cycle-HR-Nd-CS}$ was less than $\dot{Q}_{solar-cycle-Nd-CS}$ by 9.5%, 18.9%, 28.4%, 37.9%, and 47.3% due to the employment of 20%, 40%, 60%, 80%, and 100% HR.

Because of the reduction in $\dot{Q}_{solar-cycle-HR-Nd-CS}$ as compared to $\dot{Q}_{solar-cycle-Nd-CS}$, $\eta_{solar-to-fuel-HR-Nd-CS}$ was improved due to the application of HR. Table 3 reports the influence of HR on $\eta_{solar-to-fuel-HR-Nd-CS}$ of the Nd-CS cycle. From the listed numbers, it is evident that the application of HR from 20% to 100% have increased $\eta_{solar-to-fuel-HR-Nd-CS}$ significantly. For example, at TR-Nd = 40%, $\eta_{solar-to-fuel-HR-Nd-CS}$ was upsurged by 1.09%, 2.47%, 4.27%, 6.72%, and 10.26% in comparison to $\eta_{solar-to-fuel-Nd-CS}$ due to the employment of HR = 20%, 40%, 60%, 80%, and 100%, respectively. Besides, %TR-Nd and T_H required to attain a maximum $\eta_{solar-to-fuel-HR-Nd-CS}$ was reduced because of the application of HR. As the HR enhanced from 20% to 40%, 60%, 80%, and 100%, the maximum $\eta_{solar-to-fuel-HR-Nd-CS} = 10.51\%$, 11.84%, 13.61%, 16.02%, and 19.61% can be achieved at TR-Nd = 55% ($T_H = 2154$ K), 50% ($T_H = 2146$ K), 45% ($T_H = 2137$ K), 40% ($T_H = 2129$ K), and 35% ($T_H = 2120$ K), respectively.

4. Summary and conclusions

The conversion of CO_2 into solar fuels via the Nd-CS cycle was thermodynamically examined. The data required for the analysis was gathered from the HSC Chemistry 9.9 software. The equilibrium analysis indicates that to increase the TR-Nd from 15% to 30%, 45%, 60%, 75%, and 90%, T_H needs to be upsurged from 2086 K up to 2112 K,

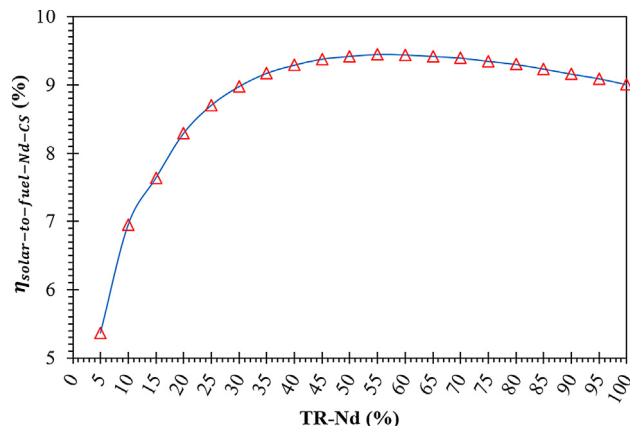


Fig. 7. Effect of %TR-Tb on $\eta_{solar-to-fuel-Nd-CS}$.

Table 3
Effect of %TR-Nd and %HR on $\eta_{solar-to-fuel-HR-Nd-CS}$.

%TR-Nd	$\eta_{solar-to-fuel-HR-Nd-CS}$ (kW)					
	HR = 0%	HR = 20%	HR = 40%	HR = 60%	HR = 80%	HR = 100%
5	5.36	6.17	7.28	8.85	11.31	15.64
10	6.95	7.91	9.17	10.91	13.48	17.61
15	7.63	8.62	9.89	11.61	14.04	17.76
20	8.29	9.33	10.67	12.47	14.98	18.78
25	8.70	9.77	11.15	12.97	15.51	19.27
30	8.97	10.06	11.45	13.27	15.79	19.50
35	9.17	10.26	11.65	13.47	15.97	19.61
40	9.29	10.38	11.76	13.56	16.02	19.55
45	9.38	10.46	11.83	13.61	16.01	19.46
50	9.42	10.49	11.84	13.59	15.94	19.27
55	9.45	10.51	11.84	13.55	15.85	19.09
60	9.44	10.49	11.79	13.47	15.70	18.82
65	9.42	10.45	11.72	13.36	15.53	18.53
70	9.40	10.41	11.66	13.26	15.37	18.27
75	9.35	10.34	11.56	13.12	15.16	17.95
80	9.30	10.27	11.48	12.99	14.97	17.67
85	9.23	10.19	11.36	12.83	14.74	17.32
90	9.16	10.09	11.23	12.66	14.50	16.98
95	9.09	10.00	11.11	12.50	14.29	16.67
100	9.00	9.89	10.97	12.31	14.03	16.31

2137 K, 2163 K, 2189 K, and 2215 K, respectively. The increment in the TR-Nd from 15% to 90% resulted in an upsurge in $\dot{Q}_{Nd_2O_3-red(partial)-Nd-CS}$, $\dot{Q}_{CO_2-heating-Nd-CS}$, $\dot{Q}_{solar-reactor-Nd-CS}$, and $\dot{Q}_{solar-heater-Nd-CS}$ by 1139.6 kW, 37.7 kW, 2188.9 kW, and 39.7 kW, respectively. Because of the rise in $\dot{Q}_{solar-reactor-Nd-CS}$, and $\dot{Q}_{solar-heater-Nd-CS}$, $\dot{Q}_{solar-cycle-Nd-CS}$ and $\dot{Q}_{re-rad-cycle-Nd-CS}$ was enhanced from 264.3 kW to 3148.4 kW and 76.5 kW to 1455.0 kW as the TR-Nd augmented from 5% to 100%. $\dot{Q}_{splitting-reactor-Nd-CS}$ was also increased from 58.4 kW up to 1167.6 kW due to the upturn in the TR-Nd from 5% to 100%. $\eta_{solar-to-fuel-Nd-CS}$ was increased from 5.36% to 9.45% as the TR-Nd upsurged from 5% to 55%. A further upturn in the TR-Nd from 55% to 100% resulted in a reduction in $\eta_{solar-to-fuel-Nd-CS}$ from 9.45% to 9.00%. With the application of HR = 100%, the Nd-CS cycle can attain a maximum $\eta_{solar-to-fuel-HR-Nd-CS} = 19.61\%$ at TR-Nd = 35% and $T_H = 2120$ K.

CRediT authorship contribution statement

Rahul R. Bhosale: Conceptualization, Methodology, Software, Validation, Formal analysis, Investigation, Resources, Data curation, Writing - original draft, Writing - review & editing, Visualization, Project administration, Funding acquisition.

Declaration of Competing Interest

The authors declare that they have no known competing financial interests or personal relationships that could have appeared to influence the work reported in this paper.

Acknowledgements

This publication was made possible by the NPRP grant (NPRP8-370-2-154) from the Qatar National Research Fund (a member of Qatar Foundation). The statements made herein are solely the responsibility of author(s).

References

- [1] Dry ME. The Fischer-Tropsch process: 1950–2000. *Catal Today* 2002;71:227–41. [https://doi.org/10.1016/S0920-5861\(01\)00453-9](https://doi.org/10.1016/S0920-5861(01)00453-9).
- [2] Figueroa JD, Fout T, Plasynski S, McIlvried H, Srivastava RD. Advances in CO₂ capture technology-The U.S. Department of Energy's Carbon Sequestration Program. *Int J Greenh Gas. Control* 2008;2:9–20. [https://doi.org/10.1016/S1750-5836\(07\)00094-1](https://doi.org/10.1016/S1750-5836(07)00094-1).
- [3] Bhosale RR, Kumar A, Almomani F, Ghosh U, Alnousse A, Scheffe J, et al. CO₂ Capture Using Aqueous Potassium Carbonate Promoted by Ethylaminoethanol: A Kinetic Study. *Ind Eng Chem Res* 2016;55:5238–46. <https://doi.org/10.1021/acs.iecr.5b04398>.
- [4] Vaidya PD, Kenig EY. CO₂-alkanolamine reaction kinetics: A review of recent studies. *Chem Eng Technol* 2007;30:1467–74. <https://doi.org/10.1002/ceat.200700268>.
- [5] Bhosale RR, Mahajani VV. Kinetics of thermal degradation of renewably prepared amines useful for flue gas treatment. *J Renew Sustain Energy* 2013;5. <https://doi.org/10.1063/1.4831960>.
- [6] Agrafiotis C, Roeb M, Sattler C. A review on solar thermal syngas production via redox pair-based water/carbon dioxide splitting thermochemical cycles. *Renew Sustain Energy Rev* 2015;42:254–85. <https://doi.org/10.1016/j.rser.2014.09.039>.
- [7] Carrillo RJ, Scheffe JR. Advances and trends in redox materials for solar thermochemical fuel production. *Sol Energy* 2017;156:3–20. <https://doi.org/10.1016/j.solener.2017.05.032>.
- [8] Bhosale RR, Takalkar G, Sutar P, Kumar A, AlMomani F, Khraisheh M. A decade of ceria based solar thermochemical H₂O/CO₂ splitting cycle. *Int J Hydrogen Energy* 2019;34–60. <https://doi.org/10.1016/j.ijhydene.2018.04.080>.
- [9] Bhosale RR, Thermochemical H₂ production via solar driven hybrid SrO/SrSO₄ water splitting cycle. *Int J Hydrogen Energy* 2019;118–27. <https://doi.org/10.1016/j.ijhydene.2018.02.053>.
- [10] Gálvez ME, Loutzenhiser PG, Hischer I, Steinfeld A. CO₂ splitting via two-step solar thermochemical cycles with Zn/ZnO and FeO/Fe₃O₄ redox reactions: Thermodynamic analysis. *Energy Fuels* 2008;22:3544–50. <https://doi.org/10.1021/ef800230b>.
- [11] Bhosale RR, Kumar A, Van Den Broeke LJP, Gharbia S, Dardor D, Jilani M, et al. Solar hydrogen production via thermochemical iron oxide-iron sulfate water splitting cycle. *Int J Hydrogen Energy* 2015;40:1639–50. <https://doi.org/10.1016/j.ijhydene.2014.11.118>.
- [12] Steinfeld A, Sanders S, Palumbo R. Design aspects of solar thermochemical engineering – a case study: two-step water-splitting cycle using the Fe₃O₄/FeO redox system. *Sol Energy* 1999;65:43–53. [https://doi.org/10.1016/S0038-092X\(98\)00092-9](https://doi.org/10.1016/S0038-092X(98)00092-9).
- [13] Koepf E, Villasmil W, Meier A. Pilot-scale solar reactor operation and characterization for fuel production via the Zn/ZnO thermochemical cycle. *Appl Energy* 2016;165:1004–23. <https://doi.org/10.1016/j.apenergy.2015.12.106>.
- [14] Bhosale RR. Thermodynamic efficiency analysis of zinc oxide based solar driven thermochemical H₂O splitting cycle: Effect of partial pressure of O₂, thermal reduction and H₂O splitting temperatures. *Int J Hydrogen Energy* 2018;43:14915–24. <https://doi.org/10.1016/j.ijhydene.2018.06.074>.
- [15] Statnatiou A, Loutzenhiser PG, Steinfeld A. Solar syngas production via H₂O/CO₂-splitting thermochemical cycles with Zn/ZnO and FeO/Fe₃O₄ redox reactions. *Chem Mater* 2010;22:851–9. <https://doi.org/10.1021/cm9016529>.
- [16] Charvin P, Abanades S, Lemont F, Flamant G. Experimental study of SnO₂/SnO/Sn thermochemical systems for solar production of hydrogen. *AIChE J* 2008;54:2759–67. <https://doi.org/10.1002/aic.11584>.
- [17] Bhosale RR, Kumar A, Sutar P. Thermodynamic analysis of solar driven SnO₂/SnO based thermochemical water splitting cycle. *Energy Convers Manag* 2017;135:226–35. <https://doi.org/10.1016/j.enconman.2016.12.067>.
- [18] Bhosale RR. Concentrated solar power driven water splitting cycle using Zn-ferrite based thermochemical redox reactions. *Int J Hydrogen Energy* 2020;45:10342–52.

- <https://doi.org/10.1016/j.ijhydene.2019.08.243>.
- [19] Scheffe JR, Li J, Weimer AW. A spinel ferrite/hercynite water-splitting redox cycle. *Int J Hydrogen Energy* 2010;35:3333–40. <https://doi.org/10.1016/j.ijhydene.2010.01.140>.
- [20] Bhosale RR, Alxneit I, Van Den Broeke LLP, Kumar A, Jilani M, Gharbia SS, et al. Sol-gel synthesis of nanocrystalline Ni-ferrite and Co-ferrite redox materials for the thermochemical production of solar fuels. *Mater. Res. Soc. Symp. Proc.* 2014;1675:203–8. <https://doi.org/10.1557/opl.2014.866>.
- [21] Bhosale RR. Thermodynamic analysis of Ni-ferrite based solar thermochemical H₂O splitting cycle for H₂ production. *Int J Hydrogen Energy* 2019;61:71. <https://doi.org/10.1016/j.ijhydene.2018.03.145>.
- [22] Bhosale R, Shende R, Puszynski J. Sol-gel synthesis of ferrite foam materials for H₂ generation from water-splitting reaction. *Nanotechnol. 2010 Adv. Mater. CNTs, Part. Film. Compos. - Tech. Proc. 2010 NSTI Nanotechnol. Conf. Expo, NSTI-Nanotech 2010, vol. 1, 2010, p. 368–71*.
- [23] Ehrhart BD, Muhich CL, Al-Shankiti I, Weimer AW. System efficiency for two-step metal oxide solar thermochemical hydrogen production – Part 1: Thermodynamic model and impact of oxidation kinetics. *Int J Hydrogen Energy* 2016;41:19881–93. <https://doi.org/10.1016/j.ijhydene.2016.07.109>.
- [24] Agrafiotis CC, Pagkoura C, Zygianni A, Karagiannakis G, Kostoglou M, Konstandopoulos AG. Hydrogen production via solar-aided water splitting thermochemical cycles: Combustion synthesis and preliminary evaluation of spinel redox-pair materials. *Int J Hydrogen Energy* 2012;37:8964–80. <https://doi.org/10.1016/j.ijhydene.2012.02.196>.
- [25] Scheffe JR, Jacot R, Patzke GR, Steinfeld A. Synthesis, characterization, and thermochemical redox performance of Hf₄+, Zr₄+, and Sc₃+ doped ceria for splitting CO₂. *J Phys Chem C* 2013;117:24104–10. <https://doi.org/10.1021/jp4050572>.
- [26] Bhosale RR, Takalkar GD. Nanostructured co-precipitated Ce_{0.9}Ln_{0.1}O₂ (Ln = La, Pr, Sm, Nd, Gd, Tb, Dy, or Er) for thermochemical conversion of CO₂. *Ceram Int* 2018;44(14):16688–97. <https://doi.org/10.1016/j.ceramint.2018.06.096>.
- [27] Takalkar G, Bhosale RR, AlMomani F. Thermochemical splitting of CO₂ using Co-precipitation synthesized Ce_{0.75}Zr_{0.25}O_{2-δ} (M = Cr, Mn, Fe, Co, Ni, Zn) materials. *Fuel* 2019;256:115834. <https://doi.org/10.1016/j.fuel.2019.115834>.
- [28] Bader R, Venstrom LJ, Davidson JH, Lipiński W. Thermodynamic analysis of isothermal redox cycling of ceria for solar fuel production. *Energy Fuels* 2013;27:5533–44. <https://doi.org/10.1021/ef400132d>.
- [29] Furler P, Scheffe JR, Steinfeld A. Syngas production by simultaneous splitting of H₂O and CO₂ via ceria redox reactions in a high-temperature solar reactor. *Energy Environ Sci* 2012;5:6098–103. <https://doi.org/10.1039/c1ee02620h>.
- [30] Le Gal A, Abanades S. Catalytic investigation of ceria-zirconia solid solutions for solar hydrogen production. *Int J Hydrogen Energy* 2011;36:4739–48. <https://doi.org/10.1016/j.ijhydene.2011.01.078>.
- [31] Carrillo RJ, Scheffe JR. Beyond Ceria: Theoretical Investigation of Isothermal and Near-Isothermal Redox Cycling of Perovskites for Solar Thermochemical Fuel Production. *Energy Fuels* 2019. <https://doi.org/10.1021/acs.energyfuels.9b02714>.
- [32] Takalkar G, Bhosale R, AlMomani F. Combustion synthesized A_{0.5}Sr_{0.5}MnO_{3-δ} perovskites (where, A = La, Nd, Sm, Gd, Tb, Pr, Dy, and Y) as redox materials for thermochemical splitting of CO₂. *Appl Surf Sci* 2019;489:80–91. <https://doi.org/10.1016/j.apsusc.2019.05.284>.
- [33] Takalkar G, Bhosale RR. Solar thermocatalytic conversion of CO₂ using PrxSr(1-x)MnO_{3-δ} perovskites. *Fuel* 2019;254. <https://doi.org/10.1016/j.fuel.2019.115624>.
- [34] Nair MM, Abanades S. Experimental screening of perovskite oxides as efficient redox materials for solar thermochemical CO₂ conversion. *Sustain Energy Fuels* 2018;2:843–54. <https://doi.org/10.1039/c7se00516d>.
- [35] Bhosale RR, Kumar A, Ashok A, Sutar P, Takalkar G, Khraisheh M, et al. La-Based Perovskites as Oxygen-Exchange Redox Materials for Solar Syngas Production. *MRS Adv.* 2017;2:3365–70. <https://doi.org/10.1557/adv.2017.300>.
- [36] Scheffe JR, Weibel D, Steinfeld A. Lanthanum-strontium-manganese perovskites as redox materials for solar thermochemical splitting of H₂O and CO₂. *Energy Fuels* 2013;27:4250–7. <https://doi.org/10.1021/ef301923h>.
- [37] Bhosale R, Kumar A, AlMomani F, Ghosh U, Anis MS, Kakosimos K, et al. Solar hydrogen production via a samarium oxide-based thermochemical water splitting cycle. *Energies* 2016;9. <https://doi.org/10.3390/en9050316>.
- [38] Bhosale RR, Kumar A, AlMomani F, Ghosh U, Khraisheh M. A comparative thermodynamic analysis of samarium and erbium oxide based solar thermochemical water splitting cycles. *Int J Hydrogen Energy* 2017;42:23416–26. <https://doi.org/10.1016/j.ijhydene.2017.03.172>.
- [39] Bhosale RR. Terbium oxide-based solar thermochemical CO₂ splitting cycle: A thermodynamic investigation. *Greenh Gases Sci Technol* 2020. <https://doi.org/10.1002/ghg.1972>.
- [40] Bhosale RR, Sutar P, Kumar A, AlMomani F, Ali MH, Ghosh U, et al. Solar hydrogen production via erbium oxide based thermochemical water splitting cycle. *J Renew Sustain Energy* 2016;8. <https://doi.org/10.1063/1.4953166>.